Poster

Characterization of spatial correlations in carbon nanotubes-modelling studies

J. Kołoczek[a], Young-Kyun Kwon[b], A. Burian[a,c,*]

[a]*Institute of Physics, University of Silesia, ul. Uniwersytecka 4, 40-007 Katowice, Poland*
[b]*Department of Physics, University of California and Materials Science Division, Lawrence Berkeley Laboratory, Berkeley, CA 94720, USA*
[c]*Centre of Polymer Chemistry, Polish Academy of Sciences, ul. M. Skłodowskiej-Curie, 41-819 Zabrze, Poland*

Abstract

The Debye equation has been used to compute the powder diffraction patterns of single- and multiwalled carbon nanotubes. By generating Cartesian coordinates of atoms the models of non-chiral and chiral nanotubes of any shape and size have been constructed. An efficient algorithm has been developed to calculate the kinematical diffraction profiles for the constructed models. The effect of curvature on the diffraction pattern has been examined by comparison of the model-based simulations for various nanotubes and a single graphene layer. The applicability of the numerical procedure is illustrated in the case of armchair, zig-zag and chiral nanotubes, both single and multiwalled. The results of the computer simulations are compared with X-ray diffraction data, recorded for multiwalled nanotubes and published recently [Szczygielska et al., Acta Phys. Polon. A 98 (2000) 611]. © 2001 Elsevier Science B.V. All rights reserved.

Keywords: Nanostructures; X-ray diffraction

1. Introduction

Up to 1985 graphite and diamond have been regarded as the only two stable crystalline forms of carbon. The works of Kroto et al. in 1985 [2] and of Iijima in 1991 [3] have resulted in the discovery of a wide family of carbon molecules, i.e. fullerenes and nanotubes. Generally these new forms of carbon have a common feature, namely all their atoms are placed on curved surfaces. In the case of fullerenes the atomic surfaces are curved in three dimensions while nanotubes exhibit two-dimensional curvature. The carbon nanotube is normally thought as a graphene sheet which is rolled into a seamless cylinder (SWNT, single-walled nanotube). When such cylinders are concentrically stacked the so-called multiwalled (or multiple walled) nanotubes (MWNT) are formed. From the geometrical point of view the carbon nanotubes can by classified as chiral and non-chiral. The non-chiral nanotubes are of two types. In the first case, the zig-zag nanotube, the tube axis is parallel to the carbon–carbon bonding lines. In the second case, the tube axis is perpendicular to the line of the C–C bond and such

constructed object is named the armchair nanotube. The non-chiral tubules exhibit a mirror symmetry plane, perpendicular to the tubule axis. A more general type of tube can be formed with a screw axis along the axis of the tubule. These are chiral tubules which show a number of helices rotating clockwise or counterclockwise (see, for example, Ref. [4]). Hamada et al. [5] introduced the notation specifying all possible rolling ways of the graphene sheet into the tubule. The two integer indices (n,m) define the tubule diameter and their chirality, respectively. In terms of this notation the armchair nanotubes are indicated by (n,n) and the zig-zag nanotubes are denoted as $(n,0)$.

Most of the existing data on the structural properties of carbon nanotubes is based on the use of electron diffraction and high resolution transmission electron microscopy (HRTEM), providing anisotropic diffraction patterns and images of the nanotubes, respectively. Although these techniques revealed important information on primary features, it is desirable to study the spatial correlations for the whole sample and this can be achieved by using the X-ray (XRD) or neutron (ND) diffraction methods. Both techniques require quite a large quantity of material however recently such quantities are available. In the present paper we report on modelling studies which result

---

*Corresponding author.
E-mail address: burian@us.edu.pl (A. Burian).

in computation of the model-based diffraction patterns. The results of such simulations are compared with existing experimental data [1].

2. Scattering formalism

X-ray and neutron diffraction experiments for carbon nanotubes can be performed only using the powder technique. When compared with the electron diffraction and HRTEM techniques both XRD and ND provide the structural information averaged over all orientations in three-dimensional space and hence lead to loss of the anisotropy of the diffraction pattern. However, from careful analysis of the powder diffraction pattern we can learn more about the structure of the nanotube as a whole. For carbon nanotubes the diffraction pattern arises from the interference of coherently scattered waves from identical scattering centres which are carbon atoms. The scattering process is usually described in terms of the structure factor $S(\mathbf{K})$ which for the system containing N atoms is expressed as

$$S(\mathbf{K}) = \frac{1}{N} \sum_{i=1}^{N} \sum_{j=1}^{N} \exp(i\mathbf{K} \cdot \mathbf{r}_{ij}) \tag{1}$$

where $\mathbf{K}$ is the scattering vector ($\mathbf{K} = \mathbf{k} - \mathbf{k_0}$), being the difference between the wave vectors $\mathbf{k}$ and $\mathbf{k_0}$ in the direction of the incident and scattered beam, respectively, and $\mathbf{r}_{ij}$ is the interatomic vector defined as the difference between the positions of the ith and jth atoms $\mathbf{r}_{ij} = \mathbf{r}_i - \mathbf{r}_j$, $k_0 = k = 2\pi/\lambda$. After averaging over all orientations one gets the so-called Debye equation [6]

$$S(K) = \frac{1}{N} \sum_{i=1}^{N} \sum_{j=1}^{N} \frac{\sin(Kr_{ij})}{Kr_{ij}}, \tag{2}$$

where $K = 4\pi \sin \theta/\lambda$, 2θ is the scattering angle and λ is the wavelength.

In order to account for the displacements of the atoms from the equilibrium positions Eq. (2) is multiplied by the Debye–Waller factor [6]

$$\exp\left(-K^2\sigma^2/2\right), \tag{3}$$

in which σ is the standard deviation of the interatomic distance. Expressing the diffraction pattern in terms of the structure factor, which is related to the normalised intensity $I(K)$ (expressed in electron units) divided by square of the carbon atomic scattering factor f^2 [7],

$$S(K) = I(K)/f^2(K), \tag{4}$$

allows for a direct comparison of the data obtained using the different diffraction techniques as XRD or ND, because $S(\mathrm{K})$ depends only on the atomic distribution (or the structure of the investigated object) and not on the atomic scattering amplitude, denoted here as f. Eq. (2) is the base of the simulation of the powder diffraction pattern, and

now, to obtain a set of interatomic distances for the particular nanotube, knowledge of the Cartesian coordinates of all the atoms forming the nanotube is required.

3. Results and discussion

Quantitative theory of the kinematical diffraction has been developed to compute the diffraction patterns of carbon nanotubes [8–11]. This approach is based on the Cochran, Crick and Vand theory of the diffraction by chiral biological molecules and leads to a closed-form expression of the intensity diffracted by the SWNTs and MWNTs of arbitrary helicity. In the present work we propose the method based on generating all possible nanotubes, both chiral and non-chiral. The model consists of a set of the Cartesian coordinates which represent all the lattice points of the nanotube. The MWNTs can be readily obtained by superposition of the individual SWNTs.

Here, we describe briefly the algorithm for the generation of the atomic coordinates of nanotubes. The basic concept of the algorithm is simply to roll a graphene sheet to make a cylinder [4]. For a nanotube to be generated, which is classified by a chiral vector $\mathbf{C}_h = (n,m)$ given with respect to the Bravais lattice vectors $\mathbf{a}_1$ and $\mathbf{a}_2$ of the graphene monolayer, one should calculate its radius $R = C_h/2\pi$, where C_h is the magnitude of $\mathbf{C}_h$ and translational vector $\mathbf{T} = (n + 2m, 2n + m)/W$, where W is the greatest common divisor of $n + 2m$ and $2n + m$. Note that the vector $\mathbf{T}$, given in the Bravais lattice vectors and perpendicular to the vector $\mathbf{C}_h$ (i.e. $\mathbf{C}_h \cdot \mathbf{T} = 0$), decides the size of the unitcell of the nanotube together with $\mathbf{C}_h$. For simplicity, the original coordinates system of the graphene sheet is transformed into a new system such that $\mathbf{T}$ is along y-axis. Then, the graphene atomic coordinates (x, y) is converted to those (X, Y, Z) of the nanotube by

$$(X,Y,Z) = \left[R\cos\left(\frac{x}{R}\right), R\sin\left(\frac{x}{R}\right), y \right]. \tag{5}$$

First the structure factors $S(K)$ have been computed for the very simple models containing about 100 atoms distributed on the cylindrical surfaces of the (5,5), (9,0) and (2,8) tubules which have the diameters of 6.78, 7.05 and 7.18 Å, respectively. The value of $\sigma = 0.05$ Å has been taken for computation in the present work. The resulting structure factors are compared in Fig. 1 with $S(K)$ computed for a single graphene layer, containing also approximately the same number of atoms. One common feature can be easily seen. All peaks for the nanotubes are shifted towards higher K values. Such shifts can be explained by shortening of the interatomic distances for the nanotubes, resulting from curvature of the tubule surface. The differences in the diffraction patterns are also clearly visible going from the armchair to zig-zag configuration. The changes are more pronounced at about 6 Å^{-1} where the
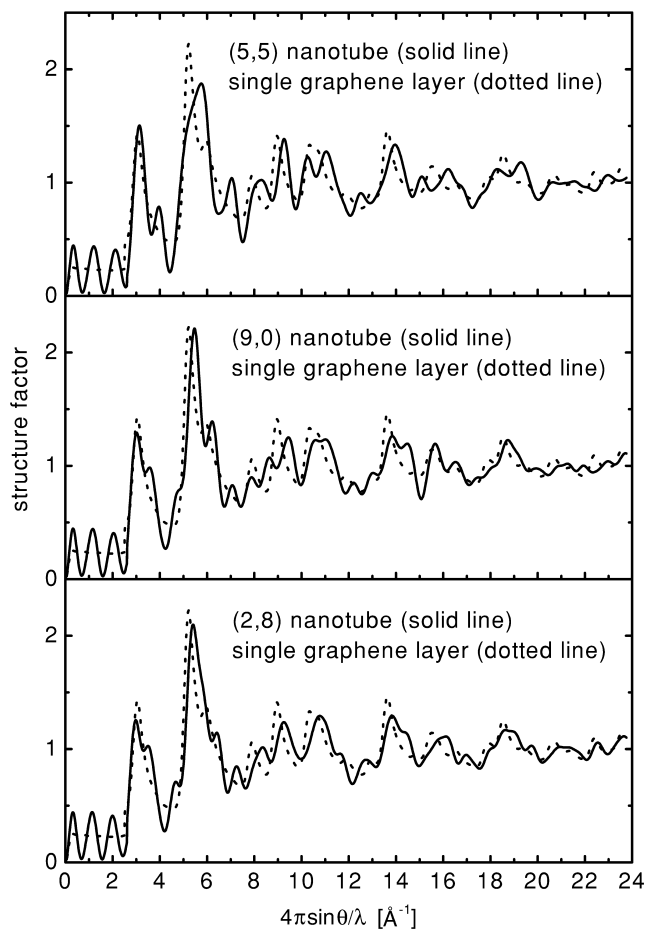
Fig. 1. The structure factors of the single walled (5,5), (9,0) and (2,8) nanotubes compared with that of a single graphene layer. Structure factors $S(K)$ were computed for the models containing about 100 atoms.
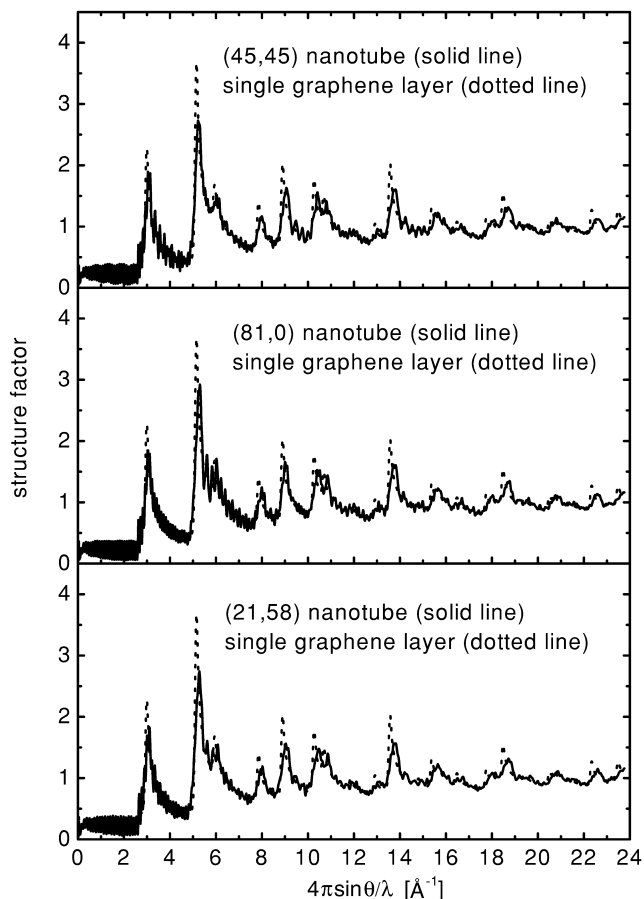

Fig. 2. The structure factors of the single walled (45,45), (81,0) and (21,58) nanotubes compared with that of a single graphene layer. Structure factors $S(K)$ were computed for the models containing about 900 atoms.

peaks have the different profiles. Remaining differences are related to slight changes in the positions and the amplitudes of the peaks. The observed differences are due to changes in spatial correlations between atoms placed on the opposite sides on the tubule circumference. The diffraction pattern of the chiral (2,8) tubule can be regarded as intermediate between two extreme cases, the armchair and zig-zag nanotubes.

These conclusions become more clear when one considers the diffraction patterns of greater nanotubes. In Fig. 2 the diffraction profiles of the (45,45), (81,0) and (21,58) nanotubes are shown together with that of a single graphene sheet. Their diameters are 61.02, 63.41 and 55.49 Å, respectively. The number of atoms for each configuration is about 900. The following features can be clearly perceived from inspection of Fig. 2. Although the diffraction patterns of the nanotubes are much closer to that of graphite than those shown in Fig. 1, the all graphitic peaks are sharper and have higher amplitudes. This observation can be explained by wider distribution of the interatomic distances within each coordination sphere in the nanotubes

due to curvature of the cylinders. The shifts of the nanotube peaks in relation to graphite are much smaller than those observed in Fig. 1 as a consequence of smaller curvature of the (45,45), (81,0) and (21,58) tubules. It is expected that in the case of the tubule of a greater diameter the effect of curvature on the diffraction pattern is much weaker. Consequently, the diffraction profiles for the three tubule configurations look very similar.

The experimentally observed carbon nanotubes are usually multiwalled. In these nanotubes the individual cylinders are separated by about 3.4–3.6 Å. The adjacent tubules consist of the different number of atoms which causes the graphitic –ABAB– stacking cannot be retained in perfect nanotubes. Moreover, the diameter of the individual tubules does not change continuously because of the quantized nature of the (*n,m*) integer indices, which determine the circumference. In Fig. 3 the experimental diffraction profile for the MWNTs, obtained by catalytic decomposition of acetylene (A type material according to Ref. [12]) is compared with a series of simulations. The experimental data were recorded on the high energy X-ray
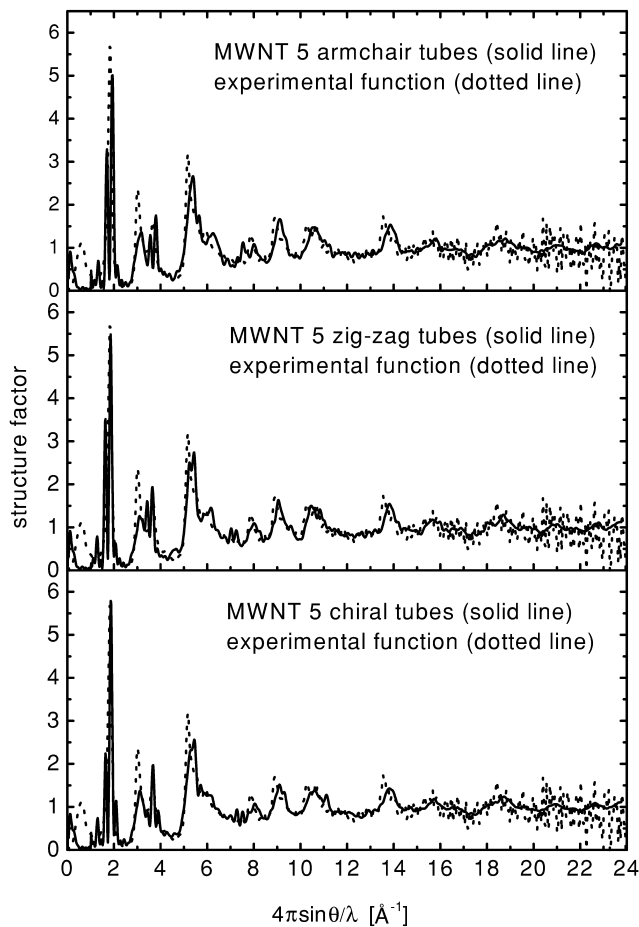
Fig. 3. Comparison of the experimental (reported in Ref. [1]) and simulated structure factors for the MWNTs. The model functions were computed for the sets of five armchair, zig-zag and chiral nanotubes (see the text).

diffraction ID15A beam line at ESRF (Grenoble, France). The detailed description of the experiment has been reported elsewhere [13].

The generated MWNTs contained five layers. The following sets were taken for computations: the (5,5), (10,10), (15,15), (20,20) and (25,25) armchair nanotubes, the (9,0), (18,0), (27,0), (36,0) and (45,0) zig-zag nanotubes and the (5,6), (4,16), (12,19), (16,23) and (8,40) chiral nanotubes. Such generated nanotubes consisted of about 1500 atoms. A fairly good agreement between the simulations and the experimental data has been achieved using this simple model, especially for the chiral nanotubes. However, it is clear that mode developed models are necessary. Splitting of the first peak, appearing at about 1.8 $\mathring{A}^{-1}$, can be related to distribution of the shortest interatomic distances for atoms laying on the adjacent cylinders. In the 3.5–24 $\mathring{A}^{-1}$ range all experimentally observed peaks are reproduced by the simulations; however, small discrepancies can be seen.

4. Summary

The computer simulations, based on the Debye equation, have shown that such an approach is able to account for all the qualitative features of the observed diffraction pattern. For the nanotubes of smaller diameter we can distinguish between different configurations. As the diameter of the tubule increases, the differences between the armchair, zig-zag and chiral nanotubes disappear. The simple model containing only five layers describes satisfactorily the atomic structure of the investigated MWNTs. Nevertheless, detailed knowledge of the structure of the nanotubes will require modelling developments to fully exploit this new opportunity. The proposed approach offers also the possibility of analysis of the experimental data in real space, because the simulated structure factor can be readily converted via Fourier transform.

Acknowledgements

References

[1] A. Szczygielska, A. Jabłońska, A. Burian, J.C. Dore, V. Honkimaki, J.B. Nagy, Acta Phys. Polon. A 98 (2000) 611.
[2] H.W. Kroto, J.R. Heath, S.C. O'Brien, R.F. Curl, R.E. Smalley, Nature 318 (1985) 162.
[3] S. Iijima, Nature 354 (1991) 56.
[4] M.S. Dresselhaus, G. Dresselhaus, P.C. Eklund, in: Science of Fullerenes and Carbon Nanotubes, Academic Press, New York, 1996.
[5] N. Hamada, S. Savada, A. Oshiyama, Phys. Rev. B 68 (1992) 1579.
[6] H.P. Klug, L.E. Alexander, in: X-ray Diffraction Procedures for Polycrystalline and Amorphous Materials, Wiley-Interscience, New York, 1974, p. 793.
[7] J.C. Dore, M. Sliwinski, A. Burian, W.S. Howells, D. Cazorla, J. Phys.: Condensed Matter 11 (1999) 9189.
[8] X.-D. Fan, L.A. Bursill, Phil. Mag. A 72 (1995) 139.
[9] A.A. Lucas, V. Bruyninckx, Ph. Lambin, Europhys. Lett. 35 (1996) 355.
[10] Ph. Lambin, A.A. Lucas, Phys. Rev. B 56 (1997) 3571.
[11] S. Amelinckx, A.A. Lucas, Ph. Lambin, Rep. Prog. Phys. 62 (1999) 1471.
[12] S. Lazarescu, Ph. Lambin, P.A. Thiry, A. Fonseca, J.B. Nagy, A.A. Lucas, Phys. Rev. B 56 (1997) 12490.
[13] A. Burian, J.C. Dore, Acta Phys. Polon. A 98 (2000) 457.